Available online at www.sciencedirect.com
ScienceDirect
Journal of Sound and Vibration 317 (2008) 456–472
JOURNAL OF SOUND AND VIBRATION
www.elsevier.com/locate/jsvi

Rapid Communication

On the use of an SPSA-based model-free feedback controller in active noise control for periodic disturbances in a duct

Ya-Li Zhou[a,*], Qi-Zhi Zhang[a], Xiao-Dong Li[b], Woon-Seng Gan[c]

[a]*Department of Computer Science and Automation, Beijing Institute of Machinery, P.O. Box 2865, Beijing 100192, People's Republic of China*
[b]*Institute of Acoustics, Academia Sinica, Beijing 100085, People's Republic of China*
[c]*School of Electronics and Electrical Engineering, Nanyang Technological University, Singapore 639798, Singapore*

Received 16 May 2008; accepted 16 May 2008
Handling Editor: L.G. Tham
Available online 26 June 2008

Abstract

In this paper, a feedback active noise control (FANC) system using a model-free (MF) controller based on simultaneous perturbation stochastic approximation (SPSA) algorithm is considered. The structure of the FANC system is first described, and the SPSA algorithm is briefly reviewed. Subsequently, the SPSA-based MF control algorithm employed in the FANC system is derived. Computer simulations are carried out to suggest that the SPSA-based MF control algorithm is effective for ANC system and much more efficient than the finite-difference stochastic approximation (FDSA) algorithm. The controller based on the SPSA-based MF control algorithm is implemented on the Texas Instruments digital signal processor (DSP) TMS320VC33. Experimental results show that the proposed scheme is able to significantly reduce periodic disturbances without the need to model the secondary path. At the same time, the simulations and the experimental verification tests also show that the convergence rate of the SPSA-based MF control algorithm is acceptable, and the SPSA-based MF control algorithm has better tracking ability under variable secondary path. This observation implies that the SPSA-based MF controller eliminates the need of modeling of the secondary path for the FANC system.

1. Introduction

Active noise control (ANC) has been the topic of much research interest in recent years [1]. Some of the research results are now finding practical applications. Typical examples are adaptive vibration damping of airplane fin structures [2], active isolation devices for ambulance transports [3], active noise control systems for air handing ducts [4], active vibration reduction for rotating rolls [5], engine sound control in leisure boats [6] and so on. Nowadays, it is possible for ANC to choose from a wide range of controllers to reject unwanted disturbances in a duct. The most common form of adaptive algorithm/architecture combination is a transversal finite impulse response (FIR) filter using the filtered-X least mean square (FXLMS) algorithm [7],

*Corresponding author.
E-mail address: zhouyali@yahoo.com (Y.-L. Zhou).

0022-460X/$ - see front matter © 2008 Elsevier Ltd. All rights reserved.
doi:10.1016/j.jsv.2008.05.027

which has been widely used in a variety of practical applications over the past decades. This controller became popular due to the ease of implementation and the high level of attenuation achievable [8,9]. But, in this control method, estimation of the secondary path is crucial to the stability of the system to generate accurate anti-noise [9].

However, characteristics of the secondary path usually vary with respect to temperature or other environments, that is, the secondary path is time variant. Therefore, it is difficult to estimate the exact characteristics of the secondary path accurately. To solve this problem, a model-free (MF) control scheme based on the simultaneous perturbation stochastic approximation (SPSA) algorithm is presented here [10]. This approach is based on the output error of the system to tune the controller coefficients without the need to model the secondary path [11]. This approach will be discussed in detail in this paper.

Meanwhile, in some applications, the reference signal is not easily available or may be expensive to measure. In these cases, feedback control should be a feasible approach [12]. Since the approach does not need measurement of the reference signal, it has been of interest for developing applicable feedback algorithms [13]. At the same time, it should be noted that feedback control is based on linear error-prediction techniques and requires periodic characteristics in the signal from the noise source [12]. Therefore, in this paper, we will only discuss the active noise control for periodic disturbances. Periodic disturbances can be widely found in rotating or reciprocating machines (such as electrical motor, pump, compressor, engine, fan, propeller, etc.) [14]. So it is very important to cancel periodic disturbances in these types of applications.

The rest of this paper is organized as follows. Section 2 shows the structure of the feedback ANC (FANC) system, and Section 3 reviews briefly the SPSA algorithm and presents the SPSA-based MF control algorithm employed in the FANC system. The simulation results using the proposed algorithm in canceling periodic disturbances are shown in Section 4. This is followed by the experimental testing of the ANC system based on the SPSA-based MF control algorithm in Section 5. Finally, the comparison between the SPSA-based MF control algorithm and the on-line secondary path estimation algorithm and further works are discussed in Section 6, and conclusions are given in Section 7.

2. The FANC system

A FANC system [7] in a duct is shown in Fig. 1, where only an error microphone is used to pick up the output error signal. The error signal $e(t)$ is processed by the ANC system to generate the control signal $u(t)$. This control signal is used to drive the canceling loudspeaker to attenuate the primary acoustic noise in the duct. Fig. 2 shows the block diagram of the FANC system using the SPSA-based MF control algorithm. The primary path $P(Z)$ is from the noise source to the error microphone, and the secondary path $S(Z)$ is from the canceling loudspeaker to the error microphone, Z is the Z-transformation operator, $x(t)$ is the noise input signal, $d(t)$ is the primary disturbance signal. The SPSA-based MF controller is used to generate an control signal $u(t)$, the frequencies $\omega_1, \ldots, \omega_n$ present in disturbance $d(t)$ can be estimated by frequency estimation algorithm such as fast Fourier transformation (FFT) frequency estimation and are used as the input signal of the controller, the error signal $e(t)$ is used to adjust the controller parameters. Note that this algorithm does not use the reference signal and the estimator of the secondary path.

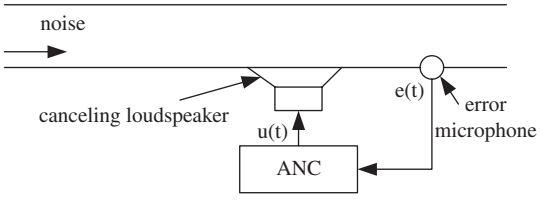

Fig. 1. Feedback ANC system in a duct.

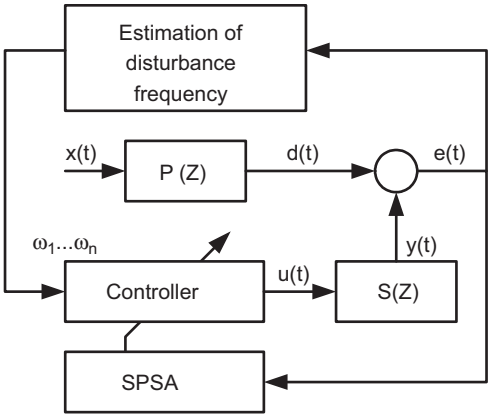

Fig. 2. Block diagram of FANC system using the SPSA-based MF controller.

3. Control algorithm

3.1. SPSA algorithm

It is known that if the secondary path of the ANC system is completely unknown, it is impossible to use usual gradient descent method (e.g., FXLMS, back-propagation neural network, etc.) as a learning rule to update the controller coefficients [4,7]. In this case, an estimator of the gradient of the error function is needed. The standard finite-difference stochastic approximation (FDSA) which was proposed by Kiefer and Wolfowitz is a well-known gradient approximation approach that relies on measurements of the objective function, not on measurements of the gradient of the objective function. However, this learning rule has a disadvantage in that it is not efficient, because the method requires $2p$ objective function measurements, where p is the number of parameters being optimized [11]. Thus, if the dimension of the parameters is large, we cannot expect viability of the learning rule in the sense of the operating speed. In order to overcome this problem, the SPSA algorithm was introduced by Spall [11]. An important feature of the SPSA is its highly efficient gradient approximation that requires only two objective function measurements regardless of the number of optimization parameters. The gradient approximation is generated by simultaneous perturbation (SP) relative to the current estimate of the parameter. Note the comparison of two function measurements versus the $2p$ measurements required in the standard FDSA approach. Therefore, the SP gradient approximation is much more efficient than the standard FDSA in terms of the amount of data required. Furthermore, it has been proven that under reasonably general conditions, SPSA and FDSA achieve the same level of statistical accuracy for a given number of iterations even though SPSA uses p times fewer function evaluations than FDSA [15]. Based on these results, the SPSA algorithm has recently been applied to many optimization problems, where it is difficult or impossible to directly obtain a gradient of the objective function with respect to the parameters being optimized.

The SPSA algorithm [15] can be described as follows. Consider the problem of finding a root θ^* of the gradient equation

$$g(\theta) \equiv \frac{\partial L(\theta)}{\partial \theta} = 0, \tag{1}$$

where θ is some p-dimensional vector of adjustable parameters, $L(\theta)$ the objective function and $g(\theta)$ the gradient of the objective function $L(\theta)$. It is assumed that only measurements of $L(\theta)$ are available and that no direct measurements of $g(\theta)$ are available.

SPSA has a standard iterative equation of

$$\hat{\theta}_{k+1} = \hat{\theta}_k - a_k \hat{g}_k(\hat{\theta}_k), \tag{2}$$

where $\hat{\theta}_k$ denotes the estimate for θ at the kth iteration, $\hat{g}_k(\hat{\theta}_k)$ represents the SP approximation to the unknown gradient $g(\theta)$ at the kth iteration, and a_k represents a scalar gain coefficient.

We have available noisy measurements of $L(\bullet)$. In particular, at design levels $\hat{\theta}_k \pm c_k\Delta_k$, let

$$y_k^{(+)} = L(\hat{\theta}_k + c_k\Delta_k) + \varepsilon_k^{(+)},$$
$$y_k^{(-)} = L(\hat{\theta}_k - c_k\Delta_k) + \varepsilon_k^{(-)}, \tag{3}$$

where ${\varepsilon_k}^{(+)}$ and ${\varepsilon_k}^{(-)}$ represent measurement noise terms [11]. The basic SP form for the estimate of $g(\bullet)$ at the kth iteration is given by

$$\hat{g}_k(\hat{\theta}_k) = \frac{y_k^{(+)} - y_k^{(-)}}{2c_k\Delta_k}, \tag{4}$$

where c_k is a positive scalar and represents a magnitude of the perturbation; $\Delta_k = \{\Delta_{k1}, \Delta_{k2}, \ldots, \Delta_{kp}\}$ is a p-dimensional random perturbation vector (typically generated by Monte Carlo), where each of the p component of Δ_k are mutual independently generated from a zero-mean probability distribution satisfying certain conditions [11]. Note that in Eq. (4), all p components of $\hat{g}_k(\hat{\theta}_k)$are updated simultaneously by the perturbation vector. So this algorithm is called SPSA. The optimal distribution for the components of the SP vector is found to be a symmetric Bernoulli ± 1 distribution with a probability of $\frac{1}{2}$ for each ± 1 outcome [16].

Taking an expectation of the quantity described in Eq. (4), from the conditions of the SP vector [17], we have

$$E(\hat{g}_k(\hat{\theta}_k)) \approx \frac{\partial L(\hat{\theta}_k)}{\partial \hat{\theta}_k}. \tag{5}$$

This equation approximates $E(\hat{g}_k(\hat{\theta}_k))$ to the derivative of the objective function $\partial L(\hat{q}_k)/\partial \hat{q}_k$ in the sense of the expected value. Therefore, this algorithm is a type of a stochastic gradient method [10,17].

3.2. SPSA-based MF control algorithm for ANC

In this section, we apply the SPSA algorithm to the ANC system. First of all, let us consider the FANC system shown in Figs. 1 and 2. The disturbance signal $d(t)$ is assumed to be

$$\begin{aligned} d(t) &= d_1 \sin(\omega_1 t + \phi_1) + d_2 \sin(\omega_2 t + \phi_2) + \cdots + d_n \sin(\omega_n t + \phi_n) \\ &= d_1^c \cos(\omega_1 t) + d_1^s \sin(\omega_1 t) + d_2^c \cos(\omega_2 t) + d_2^s \sin(\omega_2 t) + \cdots + d_n^c \cos(\omega_n t) + d_n^s \sin(\omega_n t), \end{aligned} \tag{6}$$

where $d_1, d_2, \ldots, d_n$ and $\phi_1, \phi_2, \ldots, \phi_n$ represent the amplitude and the initial phase of each frequency component of the disturbance, respectively, and are parameterized as the amplitude parameters $d_1^c, d_2^c, \ldots, d_n^c$ and $d_1^s, d_2^s, \ldots, d_n^s$; $\omega_1, \omega_2, \ldots, \omega_n$ are the frequencies of the disturbance, which can be estimated by using an FFT or the frequency selective filter (FSF), or by using a phase-locked loop before the controller is implemented. The details of frequency estimation are reported in Refs. [18,19], and are not considered in this paper. Therefore, in the following analysis, it is assumed that the frequencies $\omega_1, \ldots, \omega_n$ are known.

Thus, the control signal $u(t)$ can be expressed as

$$u(t) = f(\sin\,\omega_1 t, \sin\,\omega_2 t, \ldots, \sin\,\omega_n t, \cos\,\omega_1 t, \cos\,\omega_2 t, \ldots, \cos\,\omega_n t, \mathbf{w}). \tag{7}$$

The vector $\mathbf{w}$ includes the parameters of the controller to be estimated and can be expressed as

$$\mathbf{w} = [w^1, w^2, \ldots, w^m]^{\mathrm{T}} \tag{8}$$

where the superscript m denotes the number of parameters to be estimated, the superscript T is transpose of a vector.

The aim of the following analysis, based upon the preceding framework, is to apply the SPSA algorithm to the ANC system.

Step (1): Define the error function

Note that in ANC system, each sampling error signal does not contain enough information as an evaluation function to be optimized. That is, the expectation of the error signal has to be used as the evaluation function.

For practicality, the sum of the error signal for a certain interval is used to approximate the expectation of the error signal. Thus, the error function is defined by

$$J(u(t)) = \frac{1}{2}\sum_{t=1}^{\lambda} e^2(t) = \frac{1}{2}\sum_{t=1}^{\lambda} [y(t) + d(t) + \varepsilon(t)]^2, \tag{9}$$

where t is the sampling number in a block interval, λ is total sampling number of one block interval and $\varepsilon(t)$ represent measurement noise term.

Step (2): Generation of SP vector

The Δ_k is generated as independent Bernoulli random variables with outcomes of ± 1 and it is expressed as

$$\Delta_k = (\Delta_k^1, \ldots, \Delta_k^m)^{\mathrm{T}}. \tag{10}$$

Step (3): Error function evaluations

Obtain two measurements of the error function $J(\bullet)$ based on the SP: $J(u(w - c_k\Delta_k))$ and $J(u(w + c_k\Delta_k))$ with the Δ_k from step (2).

Step (4): Gradient approximation

Generate the SP approximation $\Delta_w(t)$ to the unknown gradient $\partial J(u(w))/\partial w$ by

$$\Delta_w(t) = \frac{J(u(w + c_k\Delta_k)) - J(u(w - c_k\Delta_k))}{2c_k\Delta_k}. \tag{11}$$

Step (5): Update the parameter vector w

$$w(t+1) = w(t) - a_k\Delta_w(t). \tag{12}$$

From Eqs. (11) and (12), it can be seen that the parameters of the ANC system are updated without the need to model the secondary path. So this algorithm is called MF control algorithm.

4. Simulation examples

In this section, some simulations are presented to illustrate the properties of the SPSA-based MF control algorithm, and at the same time, a comparison between the SPSA-based MF control algorithm and the FDSA-based MF control algorithm and the feedback FXLMS (FBFXLMS) algorithm is made. The sampling frequency used is 3 kHz, and the total sampling number of one block interval is 30. For simplicity, constant gains are used here, c_k and a_k are set as 0.001 and 0.0001, respectively. The number of iterations is 30,000.

4.1. The secondary path is linear

Case 1: First, we examine a simple problem, whereby a single major frequency $\omega_n = 300$ Hz sinusoidal signal is used as the noise input signal. Then the control signal $u(t)$ can be expressed as

$$u(t) = f(\sin\,\omega_n t, \cos\,\omega_n t, w) = c_n\,\sin(\omega_n' t + \phi_n') = c_n^c\,\cos(\omega_n' t) + c_n^s\,\sin(\omega_n' t), \tag{13}$$

where $\omega_n' = \omega_n + \delta$, δ is the offset between the frequency of the control signal $u(t)$ and the major frequency of the disturbances signal $d(t)$.

The vector $\mathbf{w}$ can be expressed as

$$\mathbf{w} = [c_n^c \quad c_n^s]^{\mathrm{T}}. \tag{14}$$

The secondary path is assumed to be time invariant, and the frequency of the control signal $u(t)$ is exactly equal to the major frequency of the disturbances $d(t)$, i.e. $\omega_n' = \omega_n$. The acoustic paths are chosen as follows:

The primary acoustic path from noise source to error microphone is [9]

$$P(Z) = 0.8Z^{-9} + 0.6Z^{-10} - 0.2Z^{-11} - 0.5Z^{-12} - 0.1Z^{-13} + 0.4Z^{-14} - 0.05Z^{-15}. \tag{15}$$

The secondary acoustic path from secondary source to error microphone is [9]

$$S(Z) = Z^{-5} + 2.5Z^{-6} + 1.76Z^{-7} + 0.15Z^{-8} - 0.4825Z^{-9} - 0.18625Z^{-10} - 0.005Z^{-11} - 0.001875Z^{-12}, \quad (16)$$

where Z^{-1} denotes unit delay and it has the effect of delaying the sampled signal by one sampling period.

Fig. 3 presents the simulation result of the canceling errors in the frequency domain. The thin solid line shows the power spectrum of active noise canceling error when the FANC system is turned off, and the thick solid line shows the power spectrum of active noise canceling error when the SPSA-based MF control algorithm is used to adapt the coefficients of the controller. From the results shown in Fig. 3, it can be clearly seen that the major disturbance frequency are attenuated greatly. The overall attenuation is prevented from going higher because only the major frequency (at $\omega = 300$ Hz) is controlled.

Case 2: Next, we deal with a tracking problem and compare the SPSA and FBFXLMS algorithms for the case where the secondary path is time variant. Using the same settings as in case 1, after the system has entered into steady-state phase, the secondary path is altered by letting $S(z) = -S(z)$. Fig. 4 shows the error signal in error microphone versus the number of iterations. When the number of iteration reaches 15,000, the secondary

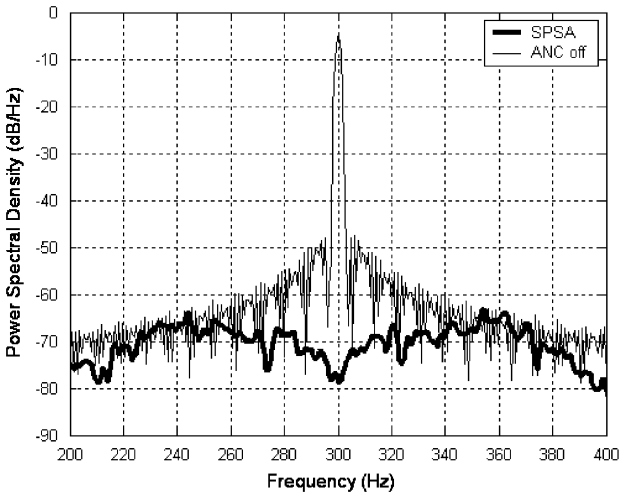

Fig. 3. Power spectrum of active noise canceling errors for case 1.

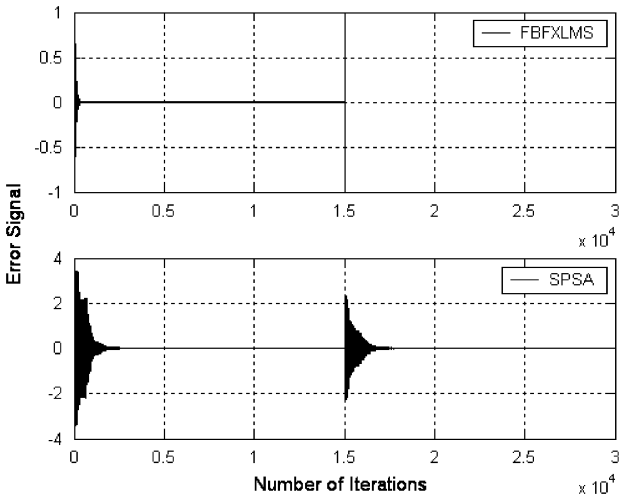

Fig. 4. Error signal versus number of iterations when the secondary path is changed.

path is changed. From the results shown in Fig. 4, it can be seen that both the SPSA-based MF control algorithm and the FBFXLMS algorithm can attenuate noise effectively. But only the SPSA-based MF control algorithm can be adapted to the change of the secondary path. This simulation shows that the SPSA-based MF controller can eliminate the need of the modeling of the secondary path for the FANC system.

Case 3: Again, using the same settings as case 1, it is assumed that there exists an offset between the frequency of the control signal and the major frequency of the disturbances. The major frequency of the disturbances $\omega_n = 300\,\text{Hz}$, and the frequency of the control signal $\omega'_n = 300.05\,\text{Hz}$. Fig. 5 shows the resultant error signal spectrum. In another frequency offset setting, $\omega'_n = 300.9\,\text{Hz}$, and the resultant error signal spectrum is shown in Fig. 6. From the results shown in Figs. 5 and 6, it can be seen that the SPSA-based MF feedback control algorithm allows less than 1 Hz offset between the frequency of the control signal and the major frequency of the disturbances. Of course, the greater the offset, the lower the cancellation noise ability.

Case 4: Finally, it is assumed that there are two major frequencies in the noise spectrum ($\omega_1 = 200\,\text{Hz}$, $\omega_2 = 300\,\text{Hz}$), and the frequency of the control signal $u(t)$ is exactly equal to the major frequency of the

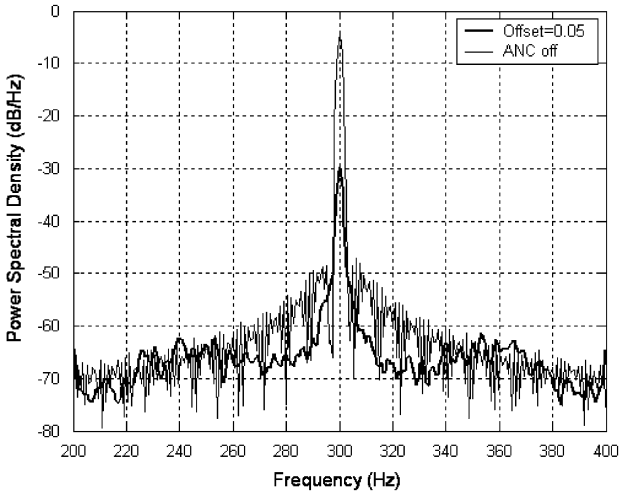

Fig. 5. Power spectrum of active noise canceling errors for offset = 0.05.

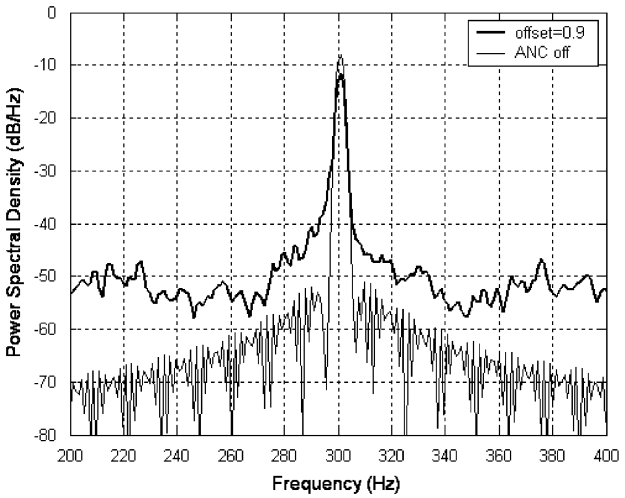

Fig. 6. Power spectrum of active noise canceling errors for offset = 0.9.

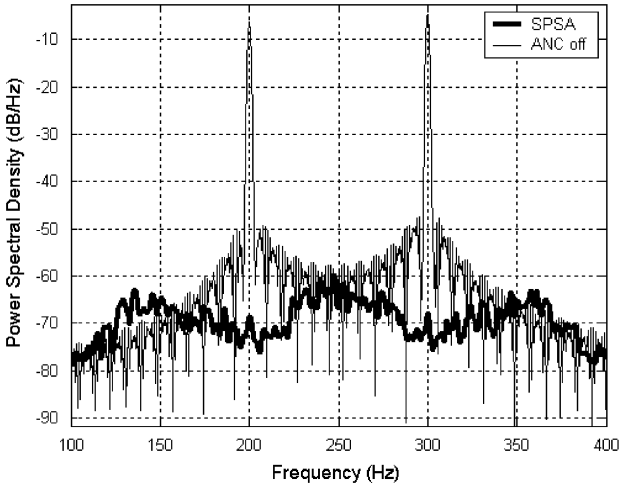

Fig. 7. Power spectrum of active noise canceling errors for case 4.

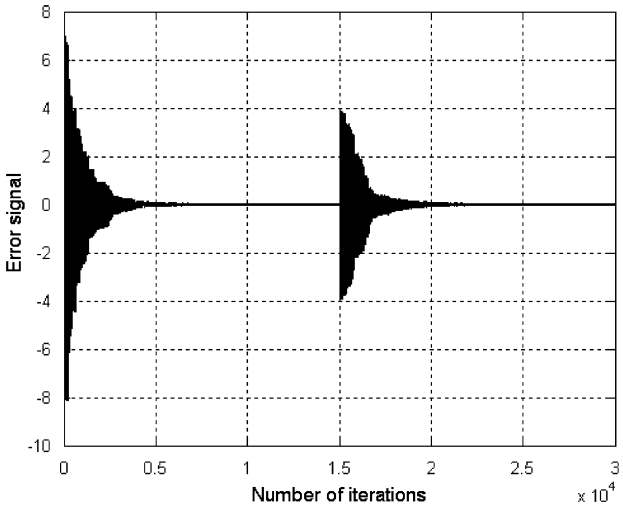

Fig. 8. Error signal versus number of iterations when the secondary path is changed.

disturbances $d(t)$. Then the control signal $u(t)$ can be expressed as

$$u(t) = f(\sin\ \omega_1 t, \sin\ \omega_2 t, \cos\ \omega_1 t, \cos\ \omega_2 t, w) = c1\ \sin(\omega_1 t + \phi_1') + c_2\ \sin(\omega_2 t + \phi_2')$$
$$= c_1^c\ \cos(\omega_1 t) + c_1^s\ \sin(\omega_1 t) + c_2^c\ \cos(\omega_2 t) + c_2^s\ \sin(\omega_2 t). \quad (17)$$

The vector $\mathbf{w}$ can be expressed as

$$\mathbf{w} = [c_1^c, c_1^s, c_2^s, c_2^s]^{\mathrm{T}}. \quad (18)$$

Other settings are the same as in case 1. Fig. 7 shows the resultant error signal spectrum, Fig. 8 shows the error signal in error microphone versus the number of iterations, when the number of iteration reaches 15,000, the secondary path is altered by letting $S(z) = -S(z)$. From the results shown in Figs. 7 and 8, it can be seen that the SPSA-based MF feedback control algorithm has good cancellation noise ability and tracking ability of the secondary path when there are two major frequencies in the noise spectrum.

4.2. The secondary path is nonlinear

When the secondary path is nonlinear, a $N_{2,6,1}$ feedforward neural network (NN) is used for the controller, which has $18+7$ weights (including thresholds) to be estimated. The inputs to the controller are $\sin\omega_n t$ and $\cos\omega_n t$, the hidden layer nodes are sigmoid functions $f(\text{net}) = (1-e^{-\text{net}})/(1+e^{-\text{net}})$, and net is the weighted sum of input signals in the input layer. The output layer node is the linear function [20,21].

The model used in this simulation has the following expressions with nonlinear terms:

The primary disturbance $d(t)$ is expressed as [22]

$$d_{t+1} = 0.8x_t + 0.6x_{t-1} - 0.2x_{t-2} - 0.5x_{t-3} - 0.1x_{t-4} + 0.4x_{t-5} - 0.05_{t-6}. \tag{19}$$

The anti-noise signal $y(t)$ is expressed as [22]

$$y_{t+1} = 0.9u_t + 0.6u_{t-1}^3 + 0.1u_{t-2}^3 - 0.4u_{t-3}^3 - 0.1u_{t-4}^3 + 0.2u_{t-5}^3 + 0.1u_{t-6}^2 + 0.01u_{t-7}^2 + 0.001u_{t-8}^2. \tag{20}$$

Case 1: A simple static ANC example is first considered to illustrate the SPSA-based MFNN algorithm effectiveness, the secondary path is assumed to be time invariant. Fig. 9 presents the simulation result of the canceling errors in the frequency domain. The thin solid line shows the power spectrum of active noise

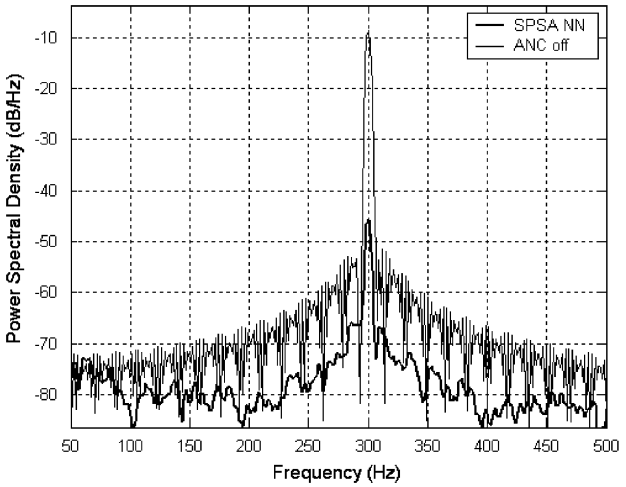

Fig. 9. Power spectrum of active noise canceling errors for case 1.

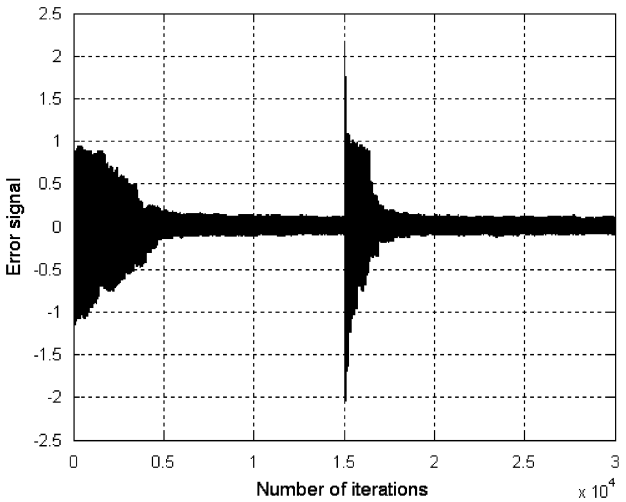

Fig. 10. Error signal versus number of iterations when the secondary path is changed.

canceling error when the ANC system is turned off, and the thick solid line shows the power spectrum of active noise canceling error when the SPSA-based MFNN algorithm is used to adapt the coefficients of the controller. From the results shown in Fig. 9, it can be clearly seen that the SPSA-based MFNN algorithm is effective for a nonlinear problem and the major disturbance frequency is attenuated approximately by 40 dB.

Case 2: Next, we deal with a tracking problem. Using the same settings as in case 1, after the system has entered into steady-state phase, the secondary path is altered by letting $S(z) = -S(z)$. Fig. 10 shows the error signal in error microphone versus the number of iterations. When the number of iteration reaches 15,000, the secondary path is changed. From the result shown in Fig. 10, it can be seen that the system has a good tracking ability of the secondary path. This simulation shows that the SPSA-based NN controller can eliminate the need of the secondary path for the FANC system.

4.3. Comparison of the SPSA and FDSA algorithms

This section compares the SPSA and FDSA algorithms for the case where the secondary path is linear. Fig. 11 shows the error signal in error microphone versus the number of iterations. Fig. 12 shows the error signal in error microphone versus the number of iterations when the number of iterations is between 9900 and 10,000. From the results shown in Figs. 11 and 12, it can be seen that the SPSA algorithm has slightly better overall performance than the FDSA algorithm, Fig. 12 illustrates that the SPSA algorithm yields a lower level of steady-state error than the standard FDSA algorithm. The critical observation to be made here is that the SPSA algorithm achieves it in performance with savings in data: each iteration of the SPSA algorithm requires only two measurements, while each iteration of the FDSA algorithm needs four measurements. Furthermore, when the neural network is used for the case where the secondary path is nonlinear, each iteration of the FDSA algorithm will need 50 measurements while each iteration of the SPSA algorithm still requires only two measurements. In consideration of the complexity of the FDSA algorithm, the comparison between SPSA and FDSA algorithms for the case where the neural network is used will not be considered here. The details about combination NN with SPSA can be found in Ref. [23]. So both theoretical and empirical evidences indicate that the SPSA algorithm is much more efficient than the standard FDSA algorithm in terms of the amount of data required. Based on the simulation results, it can be seen that the SPSA-based MF control algorithm is

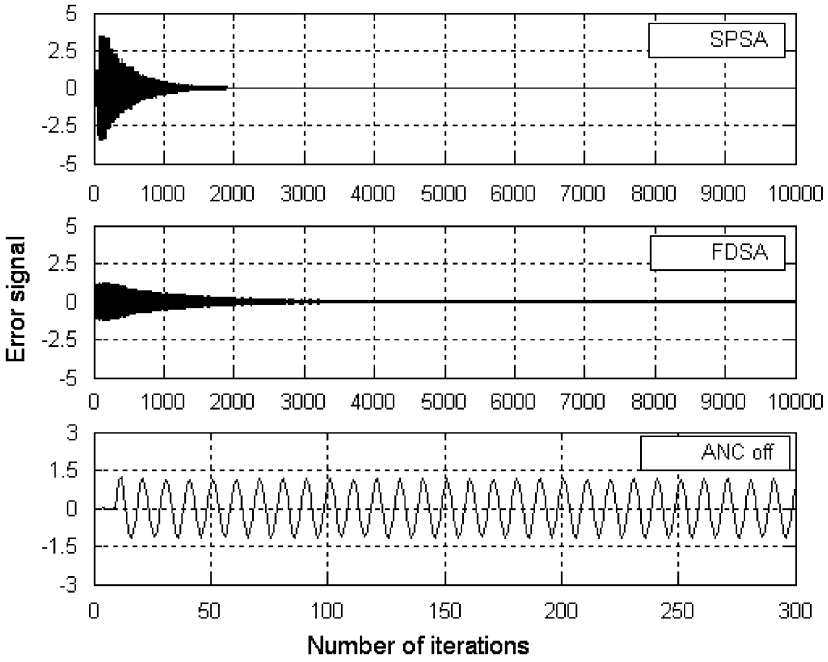

Fig. 11. Error signal versus number of iterations for the SPSA and FDSA algorithms.

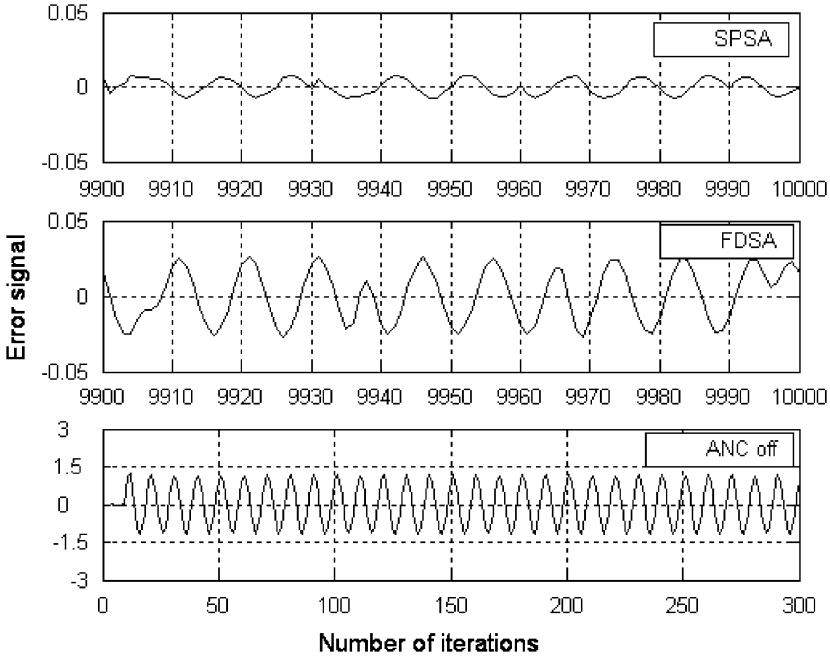

Fig. 12. Error signal versus number of iterations for the SPSA and FDSA algorithms.

effective for ANC system. Therefore, the SPSA algorithm is employed to reduce disturbances in the following experimental implementation.

5. Experimental verification

5.1. Experimental setup [9]

Now that the SPSA-based MF control algorithm used in FANC system has been derived and verified by simulations, the next step is to verify the performance in an experimental setup. The test-bed chosen for this was a simple one-dimensional duct made of wood (with two loudspeakers whose resistance is 8 Ω and diameter is 16 cm) and two PZM86 microphones. The primary loudspeaker was used to generate the primary disturbance signal, and the canceling loudspeaker was used to generate the anti-noise signal. The error microphone (♯1) was used to measure the residual error signal, and fed to DSP to adjust the controller parameters. The record microphone (♯2) was used to record the error signal and fed to the BK 3560 analyzer, which was used to analyze the error spectra. Fig. 13 shows the photo of the experimental setup, where Fig. 13a shows the duct used, and Fig. 13b is the DSP platform in which the A/D converter AD7865 and the D/A converter AD7840 are included, and Fig. 13c is the signal processing board in which the filter MAX296, the amplifier MAX422 and the switched-mode power supply HAD2.5-5-N are included. Fig. 14 shows the overall block diagram of the ANC system. The noise propagated down the duct and combined with the anti-noise signal to minimize the acoustic energy at the downstream error microphone. The length of the duct is 210 cm, and the cross section is 20 cm × 18 cm. The cutoff frequency of the duct for (1,0) mode is about 858 Hz [24]. In order to ensure that the acoustic wave propagates in the duct in the form of the plane wave, the control bandwidth was limited to 800 Hz. The controller was implemented on a TI floating-point DSP TMS320VC33 and the TI C-language was used to implement the algorithm. The error signal measured by the corresponding microphone (♯1) was first amplified by a amplifier MAX422, then filtered by a eighth-order Bessel low-pass filters MAX296 with cutoff frequency of 800 Hz and then converted from analog to digital by a AD7865, and finally processed by the DSP. The primary disturbance signal and the anti-noise signal output from DSP were first converted from digital to analog signal by AD7840, then smoothed by an eighth-order Bessel low-pass

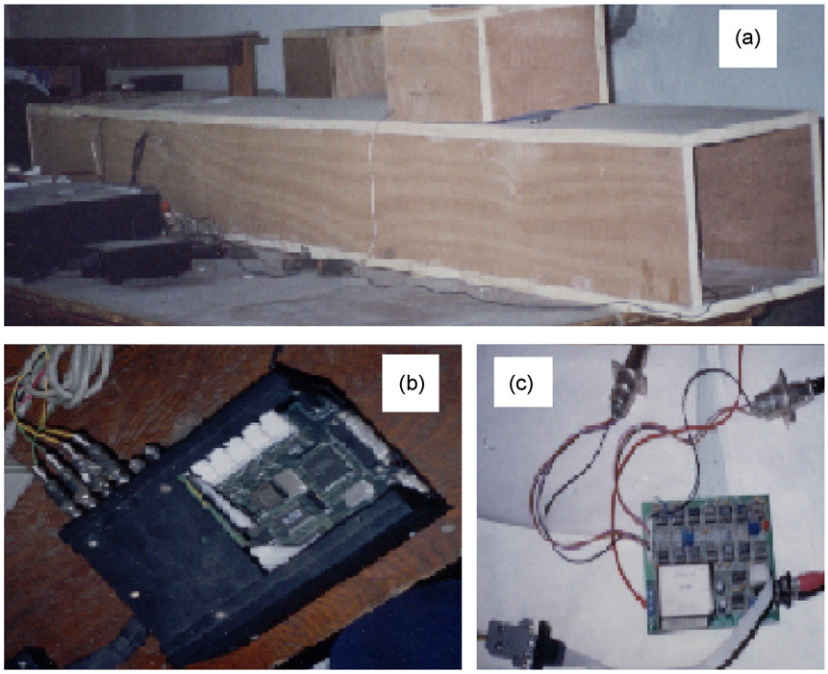

Fig. 13. The experimental duct system of active noise attenuation. (a) The duct, (b) the DSP platform, and (c) signal processing board.

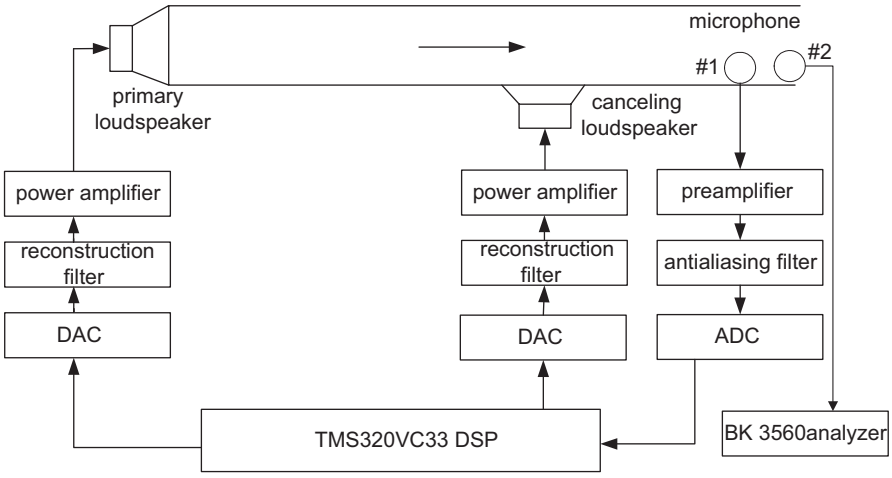

Fig. 14. The schematic diagram of active noise control system.

filters MAX296 with a cutoff frequency of 800 Hz, then amplified by the HY5885B power amplifier, which was used to drive the corresponding loudspeakers. The gain level of the preamplifier could be fine-tuned to improve its performance.

This experimental setup was selected both for convenience and simplicity. The aim of the experiments was purely to verify that the SPSA-based MF feedback control algorithm was capable of minimizing periodic disturbances.

The frequency response characteristics of the duct are shown in Figs. 15 and 16, where Fig. 15 gives the frequency response of the primary path, and Fig. 16 gives the frequency response of the secondary path.

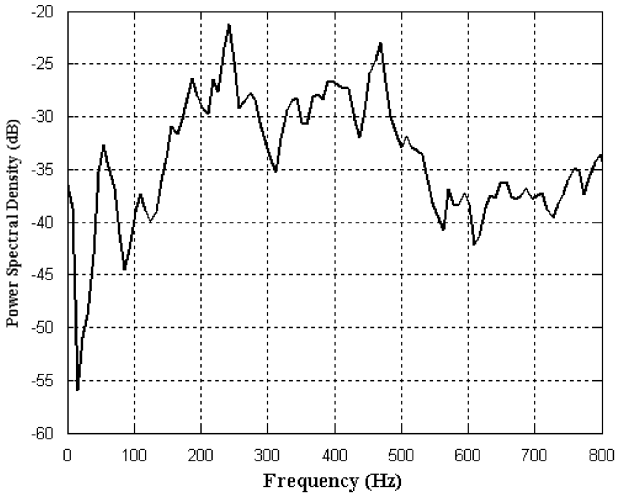

Fig. 15. Frequency response of primary path $P(Z)$.

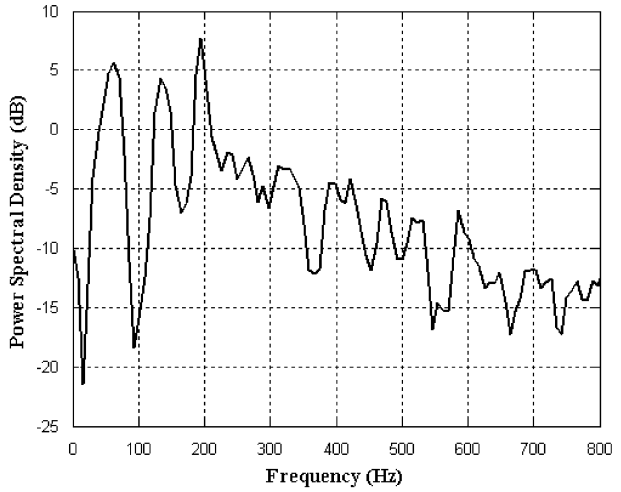

Fig. 16. Frequency response of secondary path $S(Z)$.

5.2. Active noise cancellation

The SPSA-based MF control algorithm was used to attenuate the primary noise. A 200 Hz sinusoidal signal superimposed on white noise was used as the noise input signal, the total sampling number of one block interval was 150, $c_k = 0.01$, $a_k = 0.0007$, and the sampling frequency was 10 kHz.

Case 1: The first case to consider is similar to Case 1 in Section 4.1. The secondary path is assumed to be linear and time invariant, and the frequency of the control signal $u(t)$ is exactly equal to the major frequency of the disturbances $d(t)$. The error signal spectrum during primary excitation and under control is shown in Fig. 17. From the results shown in Fig. 17, it can be seen that the major disturbance frequency 200 Hz is attenuated greatly. An output error attenuation of approximately 30 dB is achieved.

Case 2: The second case investigates the tracking ability of SPSA-based MF feedback controller. Fig. 18 shows the error signal in error microphone versus the number of iterations. From the result shown in Fig. 18, it can be seen that the convergence rate of this algorithm is acceptable. Next, similar to Case 2 in Section 4.1, after the system has entered into steady-state phase, the secondary path was changed by covering the exit of the channel with a board. Fig. 19 shows the error signal in error microphone versus the number of iterations.

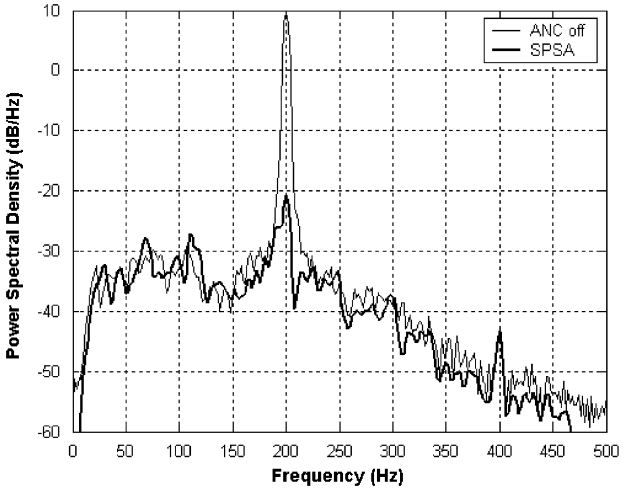

Fig. 17. Power spectrum of active noise canceling errors for case 1.

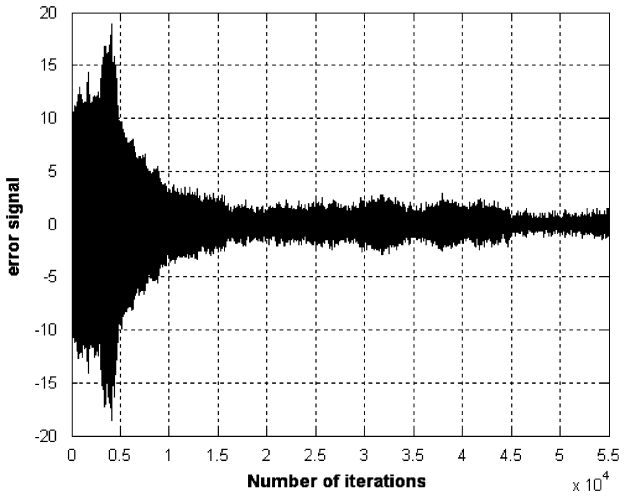

Fig. 18. Error signal versus number of iterations.

When the number of iterations is equal to about 65,000, the secondary path was changed. From the results shown in Fig. 19, it can be seen that the system has good robust performance during variation of the secondary path.

Case 3: The third case investigates the robust performance of the SPSA-based MF feedback controller when there exists an offset between the frequency of the control signal and the major frequency of the disturbances. The major frequency of the disturbances $\omega_n = 300\,\text{Hz}$, and the frequency of the control signal $\omega'_n = 300.05\,\text{Hz}$, Fig. 20 shows the resultant error signal spectrum. It can be seen that an output error attenuation of nearly 20 dB is achieved. But if the offset is larger than 0.05, it is difficult to achieve a satisfactory result. Usually, the ANC system will oscillate and go unstable, which will be discussed in the following section.

6. Discussion

The experimental results presented in the previous section clearly demonstrated the ability of the MF controller based on the SPSA algorithm to provide significant levels of noise attenuation in a feedback active

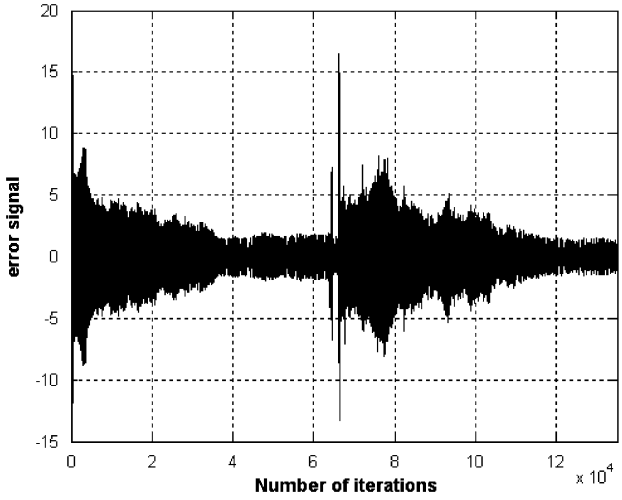

Fig. 19. Error signal versus number of iterations when the secondary path was changed.

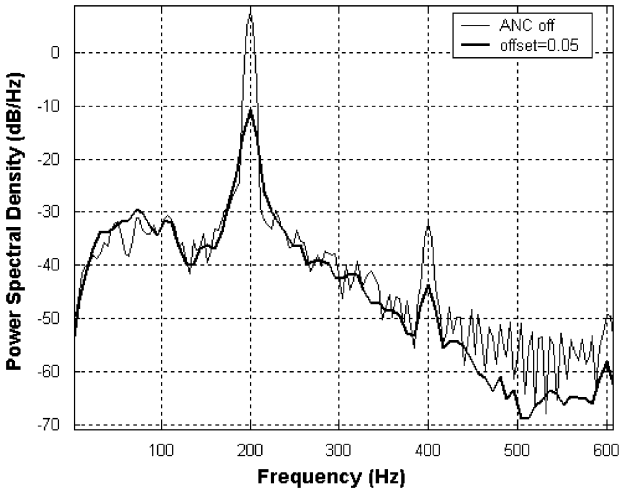

Fig. 20. Power spectrum of active noise canceling errors for offset = 0.05.

control system. From the experimental results shown in Figs. 17 and 19, it can be seen that the SPSA-based MF feedback controller can reduce periodic disturbances greatly, and eliminate the need of the modeling of the secondary path for the FANC system. Of course, the on-line secondary path modeling technique can be used when the secondary path is time variant [9,25], but one drawback to this method is that it has relatively complex structure and is computationally expensive. Furthermore, if additive random noise is introduced into the system in order to estimate the secondary path, it will affect convergence of the system and degrade the performance of the system [25]. In contrast, the MF controller based on the SPSA algorithm has a simple structure and is implementation efficient [15]. For these reasons, the SPSA-based MF control algorithm is the preferred algorithm.

The problem remaining to be solved is how to improve the offset tolerance between the frequency of the control signal and the frequency of the disturbance. A realizable suggestion is to make the frequency of the control signal self-adaptive, and also be updated by the SPSA algorithm.

7. Conclusions

This paper has presented an FANC system, for which the SPSA-based MF controller is designed. This approach optimizes error function without using derivative of the function. Therefore, the presented ANC algorithm does not require any estimation of the secondary path transfer function. Some simulations were presented to suggest that this algorithm is effective for ANC system and much more efficient than the FDSA algorithm. Following this, the MF controller based on the SPSA algorithm was implemented on a Texas Instruments DSP TMS320VC33, and was verified experimentally with a model of a duct system. The simulations and the experimental verification tests indicated that the SPSA-based MF controller was able to significantly reduce periodic disturbances without the need to model the secondary path.

Acknowledgments

This research is supported by Scientific Research Common Program of Beijing Municipal Commission of Education (KM200511232008) and Training Funds for the elitist of Beijing (20051A0500603).

References

[1] P.A. Nelson, S.J. Elliott, *Active Sound Control*, Academic Press, London, 1991.
[2] M. Stüwing, A. Büter, D. Sachau, E. Breitbach, Adaptive vibration damping of fin-structures, *Proceedings of the Seventh International Congress on Sound Vibration*, Vol. 1, Germany, 2000, pp. 123–234.
[3] U. Gnauert, D. Kohlrautz, M. Wenzel, R. Wimmel, Active isolation device for ambulance transport, *Proceedings of the Seventh International Congress on Sound Vibration*, Vol. 1, Germany, 2000, pp. 163–170.
[4] S.D. Snyder, Nobuo Tanaka, Active control of vibration using a neural network, *IEEE Transactions on Neural Networks* 6 (1995) 819–828.
[5] H. Fehren, A. Gebauer-Teichmann, U.G. Nauert, F. Grabow, H. Siebald, M. Wenzel, R. Wimmel, Active vibration reduction for rotating rolls, *Proceedings of the Seventh International Congress on Sound Vibration*, Vol. 1, Germany, 2000, pp. 379–386.
[6] M. Winberg, S. Johansson, T. Lagö, Control approaches for active noise and vibration control in a naval application, *Proceedings of the Seventh International Congress on Sound Vibration*, Vol. 1, Germany, 2000, pp. 241–248.
[7] S.M. Kuo, D.R. Morgan, *Active Noise Control Systems—Algorithms and DSP Implementations*, Wiley, New York, 1996.
[8] T. Meurers, S.M. Veres, Implementation aspects for FSF-based feedback control with secondary path estimation, *AVTIVE 2002*, ISVR, Southampton, UK, 2002, pp. 1327–1338.
[9] Y.L. Zhou, Q.Z. Zhang, X.D. Li, W.S. Gan, Analysis and DSP implementation of an ANC system using a filtered-error neural network, *Journal of Sound and Vibration* 285 (2005) 1–25.
[10] Yutaka Maeda, Takao Yoshida, An active noise control without estimation of secondary-path and using simultaneous perturbation, *ACTIVE1999*, 1999, pp. 985–994.
[11] J.C. Spall, Multivariate stochastic approximation using a simultaneous perturbation gradient approximation, *IEEE Transactions on Automatic Control* 37 (1992) 332–341.
[12] S.M. Kuo, Dipa Vijayan, Adaptive algorithms and experimental verification of feedback active noise control systems, *Institute of Noise Control Engineering* 42 (1994) 37–46.
[13] Fan Jiang, Hiroyuki Tsuji, Hiromitsu Ohmori, Akira Sano, Adaptation for active noise control, *IEEE Control Systems* 1 (1997) 36–47.
[14] Biqing Wu, Marc Bodson, Direct adaptive cancellation of periodic disturbances for multivariable plants, *IEEE Transactions on Speech and Audio Processing* 11 (2003) 538–548.
[15] J.C. Spall, Implementation of the simultaneous perturbation algorithm for stochastic optimization, *IEEE Transactions on Aerospace and Electronic Systems* 34 (1998) 817–823.
[16] Payman Sadegh, J.C. Spall, Optimal random perturbation for stochastic approximation using a simultaneous perturbation gradient approximation, *IEEE Transactions on Automatic Control* 43 (1998) 1480–1484.
[17] Yutaka Maeda, J.P. Rui, D. Figueiredo, Learning rules for neuro-controller via simultaneous perturbation, *IEEE Transactions on Neural Networks* 8 (1997) 1119–1130.
[18] Thomas Meurers, Sandor M. Veres, Stephen J. Elliott, Frequency selective feedback active noise control, *IEEE Control System Magazine* 22 (2002) 32–41.
[19] G. Chaplin, R. Smith, Method and apparatus for canceling vibration from a source of repetitive vibration, US patent 4566118, January 21, 1986.
[20] J.C. Spall, John A. Cristion, A neural network controller for systems with unmodeled dynamics with applications to wastewater treatment, *IEEE Transactions on Systems Man and Cybernetics* 27 (1997) 369–375.
[21] Y. Maeda, M. Wakamura, Simultaneous perturbation learning rule for recurrent neural network and its FPGA implementation, *IEEE Transactions on Neural Networks* 16 (2005) 1664–1672.

[22] Y.L. Zhou, Q.Z. Zhang, X.D. Li, W.S. Gan, Model-free control of a nonlinear ANC system with a SPSA-based neural network controller, *Lecture Notes in Computer Science* 3972 (2006) 1033–1038.
[23] J.C. Spall, J.A. Cristion, Model-free control of nonlinear stochastic systems with discrete-time measurements, *IEEE Transactions on Automatic Control* 43 (1998) 1198–1210.
[24] J. Hu, Jyh-Feng Lin, Feed forward active noise controller design in ducts without independent noise source measurements, *IEEE Transactions on Control System Technology* 8 (2000) 443–455.
[25] S.M. Kuo, D.R. Morgan, Active noise control: a tutorial review, *IEEE Proceedings* 87 (1999) 973–993.